

JOULE HEATING EFFECT ON ENTROPY GENERATION IN MHD MIXED CONVECTION FLOW OF CHEMICALLY REACTING NANOFLUID IN A VERTICAL CHANNEL

Md. Shafeeurrehman, D. Srinivasacharya

Department of Mathematics, Vaagdevi College of Engineering, Warangal-506005, India.

Department of Mathematics, National Institute of Technology, Warangal-506004, India.

Corresponding Author's e-mail:rahaman16@gmail.com;dsc@nitw.ac.in;

Abstract In this article the laminar mixed convective flow of an incompressible chemically reacting nanofluid in vertical channel has been investigated by considering Joule heating effect. The nonlinear governing equations are non-dimensionalized and then solved by using HAM. The entropy generation rate and Bejan number are calculated numerically. The effect of magnetic parameter, Joule heating, Brinkman number and chemical reaction parameters on the dimensionless velocity, temperature, nanoparticle concentration, entropy generation and Bejan number are investigated and represented geometrically.

Keyword: Chemical reaction, Entropy generation, HAM, Joule heating, MHD, Nanofluid.

1. Introduction

Over the past decade, nanofluids, which are conventional heat transfer fluids containing suspensions of nanometer sized particles [1], have been the subject of intensive study by the several researchers since it was reported experimentally that these fluids possess substantially higher thermal conductivity proportionate to the base fluids [1]. Nanofluids have several applications of engineering in microfluidics, microelectronics, biomedical, manufacturing, solid-state lighting, transportation, scientific measurement, material synthesis, high-power X-rays, material processing and medicine. Further, the study of mixed convective heat transfer and nanofluid flow in a vertical channel has acquired considerable attention due to its diverse application in the designs of cooling devices for electronics and microelectronic equipment, solar energy collection, etc. Number of studies were conducted on the convective heat transfer and nanofluid flow through a vertical channel by considering distinct types of conventional base fluids with particular nanoparticles. Hajipour and Dehkordi [2] analyzed the mixed convective, heat transfer of nanofluid through parallel plates. Using the Buongiorno method Hang *et al* [3] analyzed the mixed convective flow of nanofluids in a vertical channel. Nield and Kuznetsov [4] discussed the forced convection nanofluid flow in a channel. Das *et al* [5] investigated the nanoparticle volume fraction on mixed convective nanofluid flow in a vertical plates.

It is well known that the Joule heating is produced by intercommunication among the atomic ions that compose the body of the conductor and the moving charged particles that form the current. In recent years, numerous researches have been carried out for Joule heating effects. Joule heating effects on fluid flow and heat transfer at various conditions and found that it plays notable effect on MHD flow and heat transfer. Nandkeolyar *et al* [6] focused on the effects of Joule heating and viscous on nanofluid flow through a shrinking/stretching sheet

considering homogeneous–heterogeneous reactions. Zhang et al [7] conducted a numerical study on MHD fluid flow and heat transfer under different levels of thermal radiation considering Joule heating effects. Hayat et al [8] analyzed the mixed convective Jeffrey nanofluid flow in a compliant walls channel by taking Joule heating along with viscous dissipation and thermal radiation in to account.

On the other hand, the impact of chemical reaction on heat and mass transfer are of great influence in chemical technology and industries of hydrometallurgy. Chemically reacting nanofluid may play a significant role in many processing systems, materials. These include flow in packed bed electrodes, co-current buoyant upward gas-liquid [9], electrochemical generation of elemental bromine in porous electrode systems [10] Sodium Oxide-Silicon dioxide glass melt flows [11] and the manufacture of intumescent paints for fire safety applications [12]. Several investigators have focused on the effect of chemical reaction on the heat and mass transfer flowpassing through channels. Kumar et al. [13] analysed the effect of chemical reaction in a vertical parallel channel. Habibiset al.[14] study the flow reversal of chemical reacting fully developed mixed convective flow in a vertical channel. Kothandapaniet al.[15] investigated the chemical reaction effects on flow of a nanofluid in presence of inclined magnetite field in a vertical channel. Babulal and Dulalpal [16] study the combination of chemical reaction parameter and Joule heating parameter effects on MHD mixed convective flow of viscous dissipating fluid on a vertical parallel plates. Mridulkumar [17] analyses the chemical reaction effects on MHD boundary layer flow with Joule heating effect over an exponentially stretching sheet.

The amount of irreversibility associated with the real processes is measure by entropy generation. The quality of energy decreases when entropy generation takes place i.e. the entropy generation destroys the system energy. Hence, the performance of the system can be improved by decreasing the entropy generation. Therefore, a powerful and useful optimization tool for a high range of thermal applications is minimization of entropy generation. Bejan [18, 19] developed the entropy generation minimization method and introduced its applications in engineering sciences. Since then several researchers have been studying the entropy generation analysis for different types of geometries with diverse fluids. Gyftopoulos and Beretta [20] studied the entropy generation rate in a chemically reacting system. Miranda [21] studied entropy generation in a chemical reaction. Imen et al.[22] studied the entropy generation analysis of a chemical reaction process. Govindaraju et al.[23] investigated the entropy generation analysis of MHD flow of a nanofluid. The entropy generation on magnetohydrodynamic blood flow of a nanofluid influenced by thermal radiation is presented by Rashidi et al.[24]. Fersadou et al [25] analyzed numerically the entropy generation and magnetohydrodynamic mixed convective nanofluid flow in a vertical porous channel.

In many studies of heat transfer and fluid flow problems in vertical channel geometry the interactions of chemical reaction and Joule heating with nanoparticles in a mixed convection flow and entropy generation have not been considered. The main aim of this study is to examine the combined influence of chemical reaction and Joule heating on magnetohydrodynamic mixed convection flow and entropy generation due to nanofluid in vertical channel. The HAM procedure is used to solve the nonlinear differential equations. HAM [26] was first introduced by Liao, which is one of the most powerful technique to find the solution of strongly nonlinear equations. The effect of Joule heating and chemical reaction on the temperature, velocity, nanoparticle concentration, Bejan number and entropy generation is investigated.

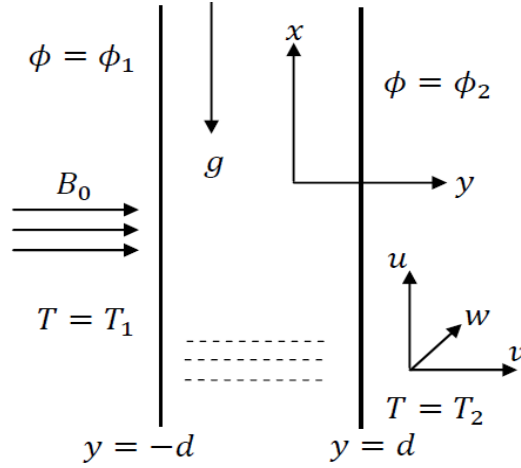


Figure 1: Geometry of the problem

2. Problem formulation

Consider a steady, laminar incompressible electrically conducting nanofluid flow through a vertical channel of width $2d$. The x -axis is taken to be in vertically upward direction of the flow through the central line of the channel and y -axis in the orthogonal direction to the flow as shown in figure 1. The temperature maintained at the plate $y=-d$ is T_1 and nanoparticle volume fraction is ϕ_1 , whereas T_2 and ϕ_2 maintained at the plate $y=d$ respectively. Rate of flow through the plates is assumed to be constant v_0 and uniformly equal for both the plates. A uniform magnetic field B_0 is taken in y -direction. A uniform pressure gradient in x -direction and buoyancy forces caused the mixed convective flow. Further, in buoyancy term the properties of fluid are taken to be constant apart from the density and the joule heating effects along with chemical reaction are taken into consideration. $u(y)$ is the velocity component in x -direction, the fluid temperature and nanoparticle volume fraction are respectively expressed by $T(y)$ and $\phi(y)$.

Under these assumptions, Equations of the conservancy of total thermal energy, mass, momentum and nanoparticle concentration with considering the nanofluid model proposed by Buongiorno[27] are as follows:

$$\frac{\partial v}{\partial y} = 0 \quad (1)$$

$$\rho_f v \frac{\partial u}{\partial y} = -\frac{\partial p}{\partial x} + \mu \frac{\partial^2 u}{\partial y^2} + (1 - \phi_m) \rho_{f_0} g \beta_T (T - T_1) - (\rho_p - \rho_{f_0}) g (\phi - \phi_1) - \sigma B_0^2 u \quad (2)$$

$$v \frac{\partial T}{\partial y} = \alpha \frac{\partial^2 T}{\partial y^2} + \frac{2\mu}{\rho c_p} \left(\frac{\partial u}{\partial y} \right)^2 + \tau \left[D_B \frac{\partial T}{\partial y} \frac{\partial \phi}{\partial y} + \frac{D_T}{T_m} \left(\frac{\partial T}{\partial y} \right)^2 \right] + \frac{1}{\rho c_p} \sigma B_0^2 u^2 \quad (3)$$

$$\frac{\partial \phi}{\partial y} v = \frac{D_T}{T_m} \frac{\partial^2 T}{\partial y^2} + D_B \frac{\partial^2 \phi}{\partial y^2} - k_l (\phi - \phi_1) \quad (4)$$

where the density is ρ , the pressure is p , D_B represents Brownian diffusion coefficient, the specific heat capacity is C_p , the viscosity coefficient is μ , β_T is the coefficients of thermal expansion, α is the effective thermal diffusivity, the acceleration due to gravity is represented by g and the thermophoretic diffusion coefficient is represented by D_T , k_l represents the coefficient of thermal conductivity. It is to be noted from (1) that $v = v_0$ (a constant).

$$\begin{aligned} u=0, \quad v=v_0, \quad T=T_1, \quad \phi=\phi_1 \quad \text{on} \quad y=-d, \\ u=0, \quad v=v_0, \quad T=T_2, \quad \phi=\phi_2 \quad \text{on} \quad y=d, \end{aligned} \quad (5)$$

Introducing the following non-dimensional variables

$$\eta = \frac{y}{d}, f = \frac{u}{u_0}, p = \frac{\mu u_0}{d^2} P, \theta = \frac{T-T_1}{T_2-T_1}, S = \frac{\phi-\phi_1}{\phi_2-\phi_1}, \quad (6)$$

in equations (1) - (5), we get the nonlinear differential equations as

$$f'' - Rf' + \frac{Gr}{Re}(\theta - NrS) + M^2 f - A = 0 \quad (7)$$

$$\theta'' - RPr\theta' + PrNb\theta'S' + PrNt\theta'^2 + 2Br(f')^2 + Jf^2 = 0 \quad (8)$$

$$S'' - RLeS' + \frac{Nt}{Nb}\theta'' - KLeS = 0 \quad (9)$$

where the kinematic viscosity coefficient is ν , $Pr = \frac{\mu C_p}{k_f}$ represents the Prandtl number

and $Le = \frac{\nu}{D_B}$ represents the Lewis number, $R = \frac{v_0 d}{\nu}$ is the suction/injection parameter,

Grashof number is $Gr = \frac{(1-\phi)g\beta_T(T_2-T_1)d^3}{\nu^2}$, $Re = \frac{u_0 d}{\nu}$ is the Reynold's number,

$M^2 = \frac{B_0^2 d^2 \sigma}{\mu}$ is the magnetic parameter, $A = \frac{d^2}{\mu u_0} \frac{\partial p}{\partial x}$ is a constant pressure gradient,

$Br = \frac{\mu u_0^2}{k_f(T_2-T_1)}$ represents the Brinkman number, the Brownian motion parameter is

$Nb = \frac{\tau D_B(\phi_2-\phi_1)}{\nu}$, $Nt = \frac{\tau D_T(T_2-T_1)}{T_m \nu}$ is the thermoporesis parameter and buoyancy ratio is

$Nr = \frac{(\rho_p - \rho_{f_0})(\phi_2 - \phi_1)}{\rho_{f_0} \beta_T(T_2 - T_1)(1 - \phi_m)}$, Joule heating parameter is $J = \frac{u_0^2 \sigma B_0^2 d^2}{(T_2 - T_1) k_f}$ and $K = \frac{k_1 d^2}{\nu}$ is the

chemical reaction parameter.

The corresponding conditions (6) on boundary are

$$\begin{aligned} S=0, \quad \theta=0, \quad f=0 \quad \text{at} \quad \eta=-1, \\ S=1, \quad \theta=1, \quad f=0 \quad \text{at} \quad \eta=1. \end{aligned} \quad (10)$$

3. Homotopy solution

To obtain the HAM solution (For more details on homotopy analysis method see the works of Liao [26,28,29, 30]), we guess the initial values as

$$f_0(\eta) = 0, \quad \theta_0(\eta) = \frac{\eta}{2} + \frac{1}{2}, \quad \text{and} \quad S_0(\eta) = \frac{\eta}{2} + \frac{1}{2}. \quad (11)$$

and the auxiliary linear operators as $L_i = \partial^2 / \partial \eta^2$, for $i = 1, 2, 3$ such that $L_1(c_1 + c_2 \eta) = 0$, $L_2(c_3 + c_4 \eta) = 0$ and $L_3(c_5 + c_6 \eta) = 0$, where $c_j, j = 1, 2, \dots, 6$ are constants.

The zeroth order deformation, which is given by

$$\begin{aligned}
(1-p)L_1[f(\eta; p) - f_0(\eta)] &= ph_1N_1[f(\eta; p)], \\
(1-p)L_2[\theta(\eta; p) - \theta_0(\eta)] &= ph_2N_2[\theta(\eta; p)], \\
(1-p)L_3[S(\eta; p) - S_0(\eta)] &= ph_3N_3[S(\eta; p)].
\end{aligned} \tag{12}$$

where

$$\begin{aligned}
N_1[f(\eta; p), \theta(\eta; p), S(\eta; p)] &= f'' - Rf' + \frac{Gr}{Re}(\theta - NrS) - M^2f - A, \\
N_2[f(\eta; p), \theta(\eta; p), S(\eta; p)] &= \theta'' - RPr\theta' + PrNb\theta'S' + PrNt\theta'^2 + 2B_r(f')^2 + Jf^2, \\
N_3[f(\eta; p), \theta(\eta; p), S(\eta; p)] &= S'' - RLeS' + \frac{Nt}{Nb}\theta'' - KLeS.
\end{aligned} \tag{13}$$

Here $p \in [0, 1]$ is the embedded parameter and $h_i, (i = 1, 2, 3.)$ are auxiliary parameters.

The equivalent boundary conditions are

$$S(-1, p) = 0, S(1, p) = 1, \theta(-1, p) = 0, \theta(1, p) = 1, f(-1, p) = 0, f(1, p) = 0. \tag{14}$$

Thus, as p varying from initial value 0 to final value 1, f , θ and S changes from f_0 , θ_0 and S_0 to the final solution $f(\eta)$, $\theta(\eta)$ and $S(\eta)$. Using Taylor's series one can write

$$\begin{aligned}
f(\eta; p) &= f_0 + \sum_{m=1}^{\infty} f_m(\eta) p^m, \quad f_m(\eta) = \frac{1}{m!} \left. \frac{\partial^m f(\eta; p)}{\partial p^m} \right|_{p=0}, \\
\theta(\eta; p) &= \theta_0 + \sum_{m=1}^{\infty} \theta_m(\eta) p^m, \quad \theta_m(\eta) = \frac{1}{m!} \left. \frac{\partial^m \theta(\eta; p)}{\partial p^m} \right|_{p=0}, \\
S(\eta; p) &= S_0 + \sum_{m=1}^{\infty} S_m(\eta) p^m, \quad S_m(\eta) = \frac{1}{m!} \left. \frac{\partial^m S(\eta; p)}{\partial p^m} \right|_{p=0}.
\end{aligned} \tag{15}$$

And choose the values of the auxiliary parameters for which the series (15) are convergent at $p=1$ i.e.,

$$f(\eta) = f_0 + \sum_{m=1}^{\infty} f_m(\eta), \quad \theta(\eta) = \theta_0 + \sum_{m=1}^{\infty} \theta_m(\eta), \quad S(\eta) = S_0 + \sum_{m=1}^{\infty} S_m(\eta). \tag{16}$$

The m^{th} -order deformation is given by

$$\begin{aligned}
L_1[f_m(\eta) - \chi_m f_{m-1}(\eta)] &= h_1 R_m^f(\eta), \\
L_2[\theta_m(\eta) - \chi_m \theta_{m-1}(\eta)] &= h_2 R_m^\theta(\eta), \\
L_3[S_m(\eta) - \chi_m S_{m-1}(\eta)] &= h_3 R_m^S(\eta).
\end{aligned} \tag{17}$$

where

$$\begin{aligned}
R_m^f(\eta) &= f'' - Rf' + \frac{Gr}{Re}(\theta - NrS) - M^2f - (1 - \chi_m)A, \\
R_m^\theta(\eta) &= \theta'' - RPr\theta' + PrNb \sum_{n=0}^{m-1} \theta'_{m-1-n} S'_n + PrNt \sum_{n=0}^{m-1} \theta'_{m-1-n} \theta'_n \\
&\quad + 2Br \sum_{n=0}^{m-1} f'_{m-1-n} f'_n + J \sum_{n=0}^{m-1} f_{m-1-n} f_n, \\
R_m^S(\eta) &= S'' - RLeS' + \frac{Nt}{Nb} \theta'' - KLeS.
\end{aligned} \tag{18}$$

for an integer m

$$\begin{aligned}
\chi_m &= 0 \quad \text{for } m \leq 1 \\
&= 1 \quad \text{for } m > 1
\end{aligned} \tag{19}$$

4. Convergence

In HAM, it is essential to see that the series solution converges. Also, the rate of convergence of approximation for the HAM solution mainly depend on the values of h . To find the admissible space of the auxiliary parameters, h -curves are drawn for 20th-level of approximation and shown in figure 2. It is observed from this figure that the permissible range for h_1 , h_2 and h_3 is $-0.6 < h_1 < -0.2$, $-0.5 < h_2 < -0.1$ and $-1.4 < h_3 < -0.2$, respectively.

In order to obtain the optimal values of the auxiliary parameters, the following average residual errors [29] are computed and found that these errors are least at $h_1=-0.43$, $h_2=-0.38$ and $h_3=-1.16$.

$$E_{f,m} = \frac{1}{2k} \sum_{i=-k}^k \left(N_1 \left[\sum_{j=0}^m f_j(i\Delta t) \right] \right)^2, E_{\theta,m} = \frac{1}{2k} \sum_{i=-k}^k \left(N_2 \left[\sum_{j=0}^m \theta_j(i\Delta t) \right] \right)^2, \quad (20)$$

$$E_{S,m} = \frac{1}{2k} \sum_{i=-k}^k \left(N_3 \left[\sum_{j=0}^m S_j(i\Delta t) \right] \right)^2.$$

where $\Delta t = \frac{1}{k}$ and $k = 5$. Also, for different values of m the series solutions are calculated and noticed that the series (16) converges in the total area of η . Further, the graphs of the ratio

$$\beta_f = \left| \frac{f_m(h)}{f_{m-1}(h)} \right|, \quad \beta_\theta = \left| \frac{\theta_m(h)}{\theta_{m-1}(h)} \right|, \quad \beta_S = \left| \frac{S_m(h)}{S_{m-1}(h)} \right|. \quad (21)$$

in contrast to the number of terms m in the homotopy series are calculated and observed that the series (16) converges to the exact solution.

5. Entropy generation

The volumetric rate of local entropy generation of the nanofluid in vertical channel can be expressed as

$$S_G = \frac{K_f}{T_1^2} \left(\frac{\partial T}{\partial y} \right)^2 + \frac{\sigma B_0^2 u^2}{T_1} + \frac{2\mu}{T_1} \left(\frac{\partial u}{\partial y} \right)^2 + \frac{RD}{\phi_1} \left(\frac{\partial \phi}{\partial y} \right)^2 + \frac{RD}{T_1} \left(\frac{\partial T}{\partial y} \right) \left(\frac{\partial \phi}{\partial y} \right) \quad (22)$$

where R universal gas constant and D is the species diffusivity through the fluid.

The entropy generation number N_s is the ratio of the volumetric entropy generation rate to the characteristic entropy generation rate according to Bejan[16]. Therefore N_s is given by

$$N_s = \theta'^2 + \frac{1}{\Omega_1} (2B_r f'^2 + J f'^2) + \phi_2 S'^2 + \phi_3 \theta' S' \quad (23)$$

The dimensionless coefficients are ϕ_2 and ϕ_3 , called irreversibility distribution ratios which are related to diffusive irreversibility,

$$\text{given by} \quad \phi_2 = \frac{RD}{K_f \Omega_1} \left(\frac{\Omega}{\Omega_1} \right) \Delta \phi, \quad \phi_3 = \frac{RD}{K_f \Omega_1} \Delta \phi \quad (24)$$

where $\Omega = \frac{\Delta \phi}{\phi_1}$, $\Omega_1 = \frac{\Delta T}{T_1}$ are the concentration and temperature ratios, respectively and

$\frac{K_f (\Delta T)^2}{d^2 T_1^2}$ is the characteristic entropy generation rate. The Eq.(23) can be expressed as

$$N_s = N_h + N_v \quad (25)$$

The entropy generation due to heat transfer irreversibility is denoted by the first term on the right hand side of the eq.(25) and the entropy generation due to viscous dissipation is represented by second term of eq.(25). The ratio of the entropy generation (N_s) and the total entropy generation (N_s+N_v) is called Bejan number (Be). To understand the entropy generation mechanisms the Bejan number Be is specified. The Bejan number for this problem can be expressed as

$$Be = \frac{N_s}{N_h + N_v} \quad (26)$$

In general the limits of Bejan number is 0 to 1. Finally, the irreversibility due to viscous dissipation dominant represent by $Be = 0$, whereas $Be = 1$ represents the domination of heat transfer irreversibility on N_s . It is clear that the heat transfer irreversibility is equal to viscous dissipation at $Be=0.5$.

6. Results and discussion

The effects of chemical reaction, Joule heating, magnetic and Brinkman number on non-dimensional velocity, temperature and nanoparticle volume fraction, Bejan number Be and entropy generation N_s are presented graphically in figures 3 - 8. To study these effect of these parameters taking computations as $Nr = 1$, $Nb = 0.3$, $Gr = 10$, $Re = 2$, $R = 1$, $Pr = 1$, $A = 1$, $Le = 1$, $Tp = 0.1$

Figure 3 displays the impact of the chemical reaction K on velocity, dimensionless temperature, nanoparticle volume fraction. Figure (3a) reveals that the velocity increase as an enhance in the chemical reaction K . This indicates that K have a retarding impact on the mixed convective flow. From figure (3b), it is noticed that $\theta(\eta)$ increased with an increment in the parameter K . The influence of parameter K is to raise the temperature extremely in the flow field. From the flow region the heat energy released because of a raise in the chemical reaction therefore the fluid temperature increases. It is evident from figure (3c) that the nanoparticle concentration $S(\eta)$ decays with a raise in the parameter K .

The influence of the Joule heating parameter J on the velocity $f(\eta)$, temperature $\theta(\eta)$ and nanoparticle volume fraction $S(\eta)$ is shown in Figure 4. The dimensionless velocity $f(\eta)$ raises with the rise in Joule heating parameter J as shown in figure (4a). Figure (4b) reveals that the temperature enhanced with an increment in Joule heating parameter J . From figure (4c) it is noticed that nanoparticle concentration $S(\eta)$ decay with growth in Joule heating parameter J .

Figure 5 represents the influence of the chemical reaction K on Bejan number Be and entropy generation. Figure (5a) shows that entropy generation enhanced with enhance in the chemical reaction parameter K . It is clear from Figure (5b) that Be (Bejan number) increasing near the lower plate of the channel, meanwhile far away from the plate the trend is reversed due to more contribution of the heat transfer irreversibility on N_s and Be decreasing at upper plate of the channel as enhance in K .

The influence of magnetic parameter M on Bejan number Be and entropy generation N_s is presented in figure 6. Figure (6a) shows that entropy generation decay with growth in the magnetic parameter M . From the figure (6b) it is clear that Be increased near the lower plate of the channel, meanwhile far away from the plate the trend is reversed due to more contribution of the heat transfer irreversibility on N_s and Be decreasing at upper plate of the channel as enhance in the value of M .

The effects of the Brinkman number Br and Joule heating parameter J on Bejan number Be and entropy generation Ns is displayed in figure 7. Figure (7a) shows that the enhance in Br causes an increment in entropy generation. As increase in Brinkman number Br the Bejan number is observed as increasing near the end plate of the channel, while the trend is reversed at centre of the channel due to more contribution of heat transfer irreversibility on Ns and Be increasing near the upper plate of the channel as represented in figure (7b).

Figure 8 reveals the impact of the Brinkman number Br and Joule heating parameter J on Bejan number Be and entropy generation Ns . Figure (8a) shows that the enhance in the parameter J causes a increment in entropy generation. As increase in J the Bejan number is observed as decreasing near the lower plate of the channel, meanwhile far away from the plate the trend is reversed due to more contribution of heat transfer irreversibility on Ns and Be increasing near the upper plate of the channel as represented in figure (8b).

7. Conclusions

In this article the laminar entropy generation in mixed convective nanofluid flow in a vertical channel has been investigated by including magnetic, Joule heating, Brinkman number and chemical reaction parameter effects. The non-dimensional non-linear equations are solved by the HAM procedure. The main decision are encapsulate below:

- The dimensionless velocity, temperature and entropy generation increases whereas the nanoparticle concentration decreased with raise in chemical reaction parameter K .
- The dimensionless temperature, velocity and entropy generation increases but the nanoparticle concentration decreases as the parameter J increases.
- The maximum values of Bejan number are observed at upper and lower plate of the channel due to more contribution of heat transfer irreversibility on Ns by increasing the effects of parameters K , M , Br , J and Nt .

References

- [1]. S.U.S. Choi, *ASME MD*, 231(1995) 99–105.
- [2]. M. Hajipour, A.M. Dehkordi, *Int. J. Thermal Sciences*.55 (2012) 103-113.
- [3]. X. Hang, F. Tao, I. Pop, *Int. Commun. Heat Mass Trans.* 44 (2013) 15-22.
- [4]. D.A. Nield, A.V. Kuznetsov, *Int. J. Heat Mass Trans.* 70 (2014) 430-433.
- [5]. S. Das, R.N. Jana, O.D. Makinde, *Eng. Sci. Tech. an Int. J.* 18 (2015) 244-255.
- [6]. R. Nandkeolyar, S. S. Motsa and P. Sibanda, *J. of Nanotech. Eng. and Med* 4, (2013) 1-9.
- [7]. J. K. Zhang, B. W. Li and Y. Y. Chen, *J. of Heat Transfer* 137(2015) 1–10.
- [8]. T. Hayat, Maryam Shafique, A. Tanveer, A. Alsaedi, *J. of Magnetism and Magnetic Materials* 407(2016) 51–59.
- [9]. K. Takahashi and R. Alkire. . *Chem. Eng. Commun.*, 38 (1985).
- [10]. J. Qi and R. F. Savinell., *J. Applied Electrochemistry* 23(1993) 873 – 886.
- [11]. Y. A. Guloyan. *Glass and Ceramics*.60 (2003).
- [12]. P. Ducrocq, S. Duquesne, S. Magnet, S. Bourbigot, and R. Delobel. *Progress in Organic Coatings*.,57 (2006) 430- 438.
- [13]. J.P. Kumar, J.C. Umavathi, J. Sharadkumar, *Int. J. of Eng. Res.&Appl* 3(2013) 967-977.
- [14]. H. Saleh, H. Ishak, S. Basriati, *Int. J. of Chem. Eng.* 2013.
- [15]. M. Kothandapani, J. Prakash, *Asia-Pac. J. Chem. Eng.* 10 (2015) 259–272.
- [16]. P. Dulal, T. Babulal, *Math. Comp. Modelling* 54 (2011).
- [17]. G. Mridulkumar *Int. Res. J of Eng. Tech. (IRJET)* 2 (2015).
- [18]. A. Bejan, *Entropy generation through heat and fluid flow*. New York: Wiley; 1996.
- [19]. A. Bejan, *Entropy generation minimization*. New York: Wiley; 1982.
- [20]. E. P. Gyftopoulos, G. P. Beretta, *J. of Egy Resources Tech.* 115(1993).
- [21]. E. N. Miranda, *Eur. J. Phys.* 31(2010) 267–277.
- [22]. Ch. Imen, H. Nejib, B. B. Ammar, *J. of Heat Trans.* 136(2014).
- [23]. M. Govindaraju, G. N. Vishnu, B. Ganga, H. A. K. Abdul, *J. of Egyp. Math. Society* 23 (2015) 429–434.
- [24]. M. M. Rashidi, M. M. Bhatti, M. A. Abbas, M. El-Sayed Ali, *Entropy* 18 (2016).
- [25]. I. Fersadou, H. Kahalerras, M. El Ganaoui, *Computers & Fluids* 121(2015) 164-179.
- [26]. S. J. Liao, *Beyond perturbation. Introduction to homotopy analysis method*, Boca Raton: Chapman and Hall/CRC Press (2003).
- [27]. J. Buongiorno, *ASME J Heat Transfer* 128 (2006) 240 – 250.
- [28]. S. J. Liao, *Appl. Math. Comp.* 147(2004) 499–513.
- [29]. S. J. Liao, *Commun. Nonlinear Sci. Numer. Simul.* 15(2010).
- [30]. S. J. Liao, *Advances in the Homotopy Analysis Method*. World Scientific Publishing Company, Singapore. (2013).

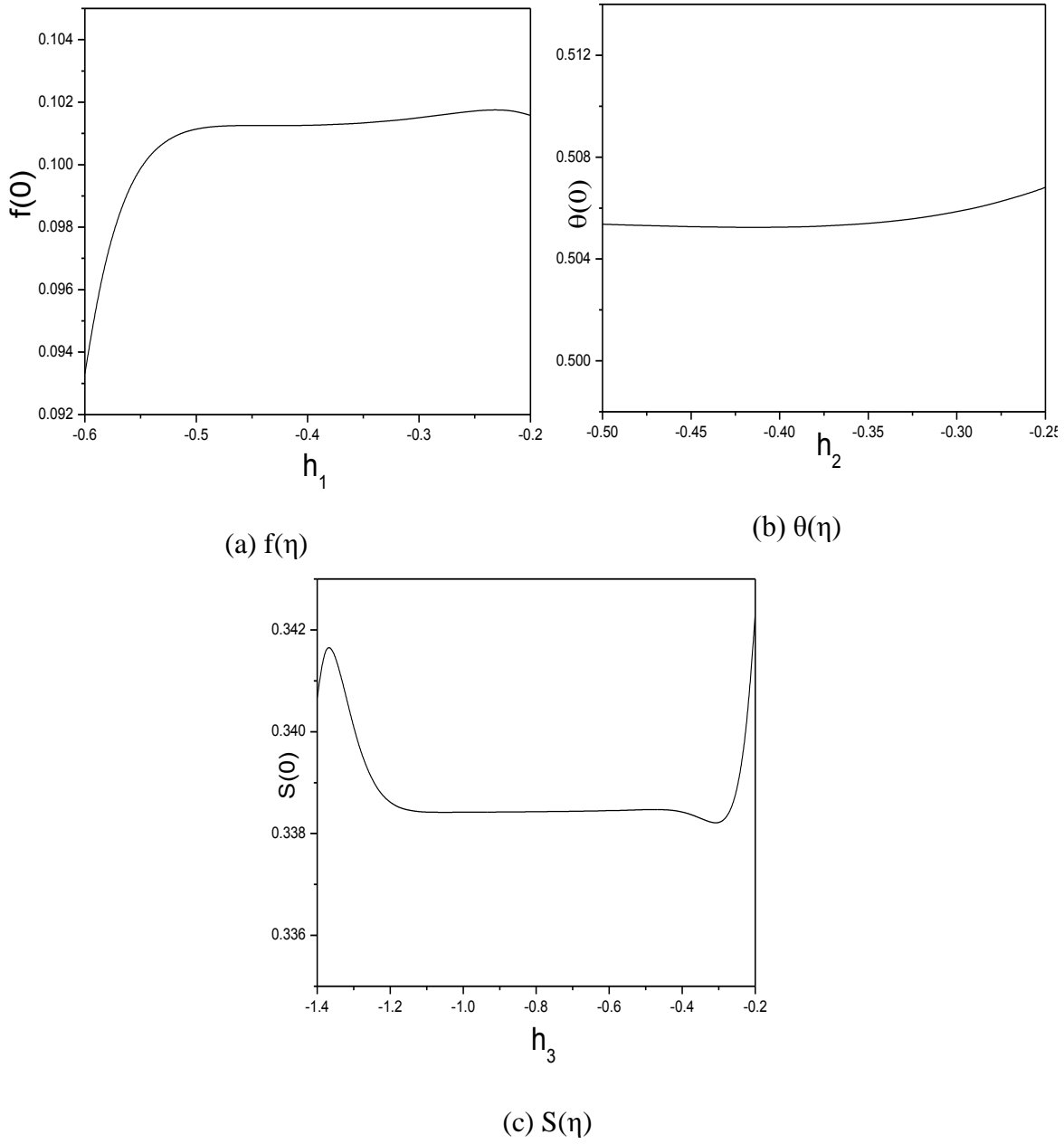


Figure 2: The h-curves for $f(\eta)$, $\theta(\eta)$, $S(\eta)$ when $Nr = 1, Nt = 1, Gr = 10, R = 1, Nb = 0.5$, $Pr = 1, A = 1, Re = 2, Le = 1, Rd = 1.5, M = 2, Br = 0.5, J = 2, Tp = 0.1$.

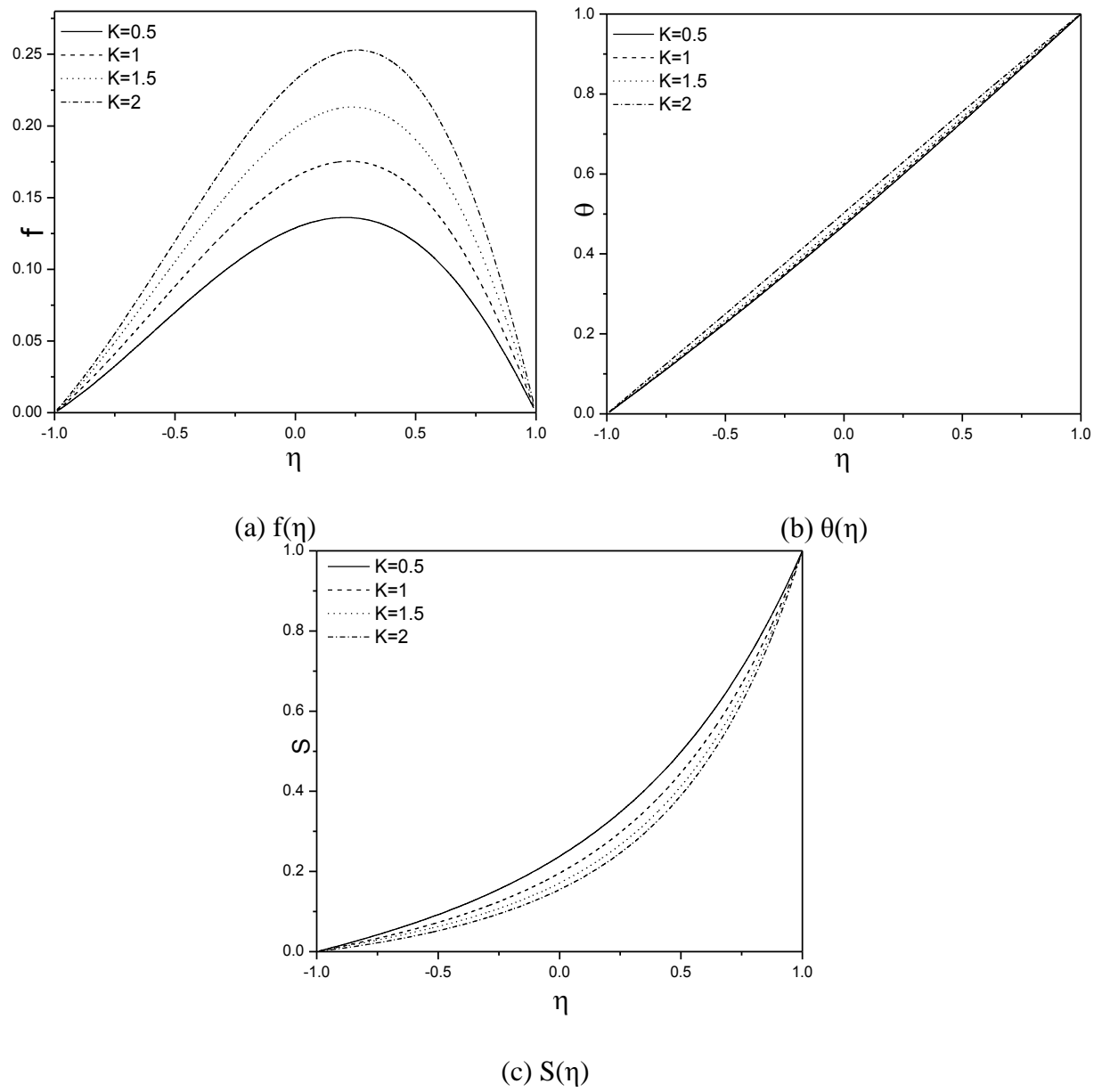


Figure 3: Effect chemical reaction on velocity $f(\eta)$, temperature $\theta(\eta)$ and nanoparticle concentration $S(\eta)$.

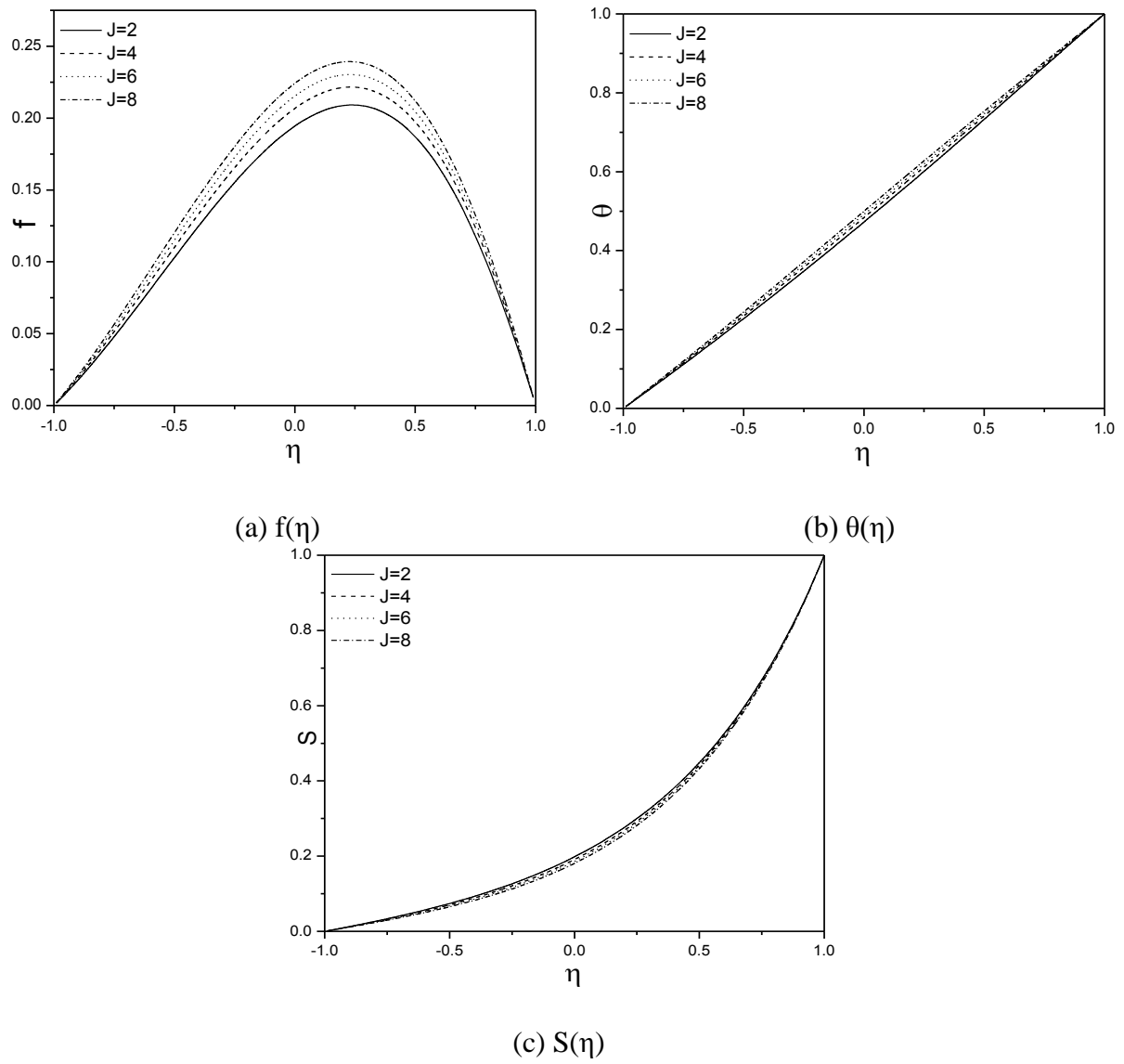
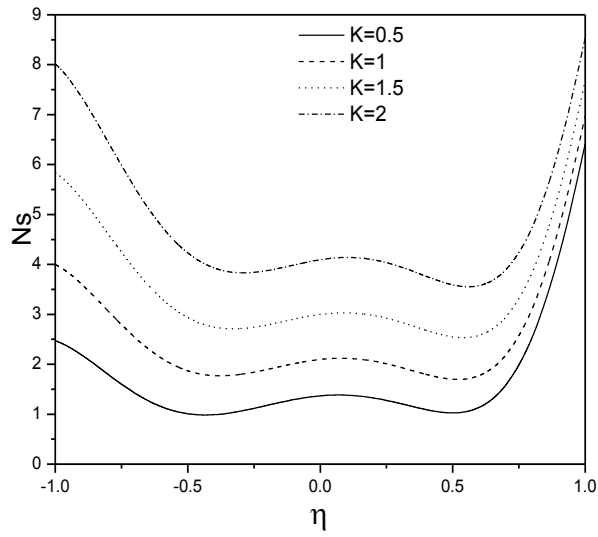
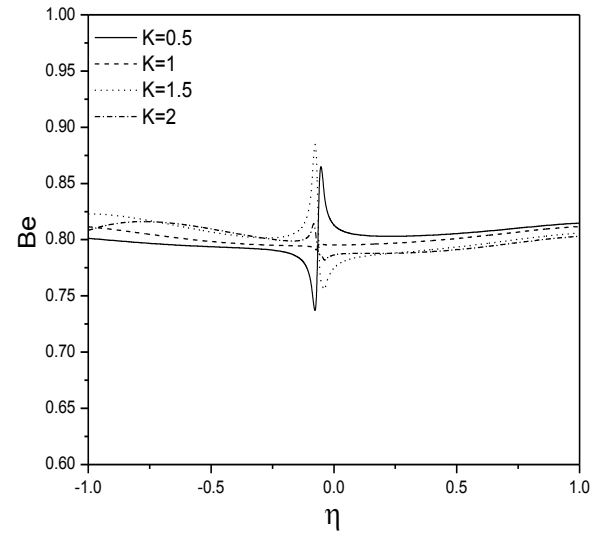


Figure 4: Effect of Joule heating parameter on velocity $f(\eta)$, temperature $\theta(\eta)$ and nanoparticle concentration $S(\eta)$.

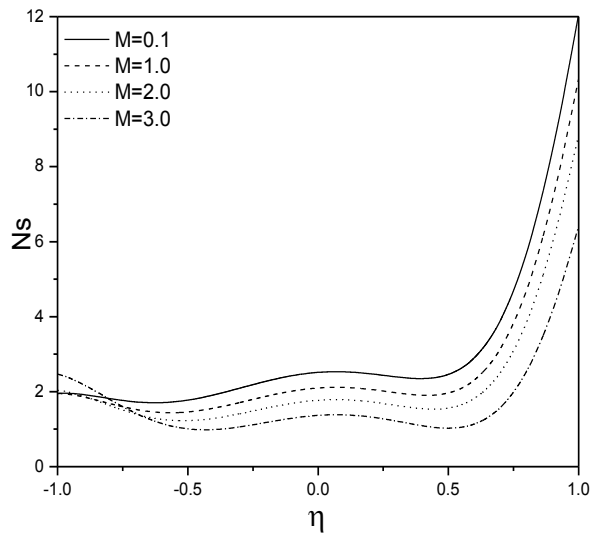


(a) $Ns(\eta)$

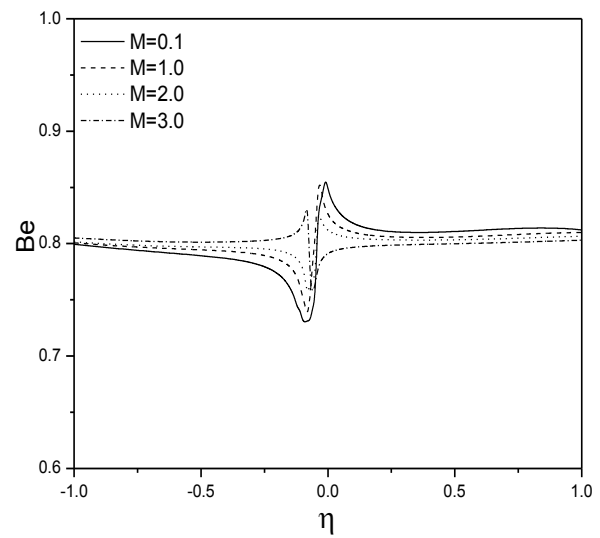


(b) $Be(\eta)$

Figure 5: Effects of chemical reaction parameter on entropy generation and Bejan number.

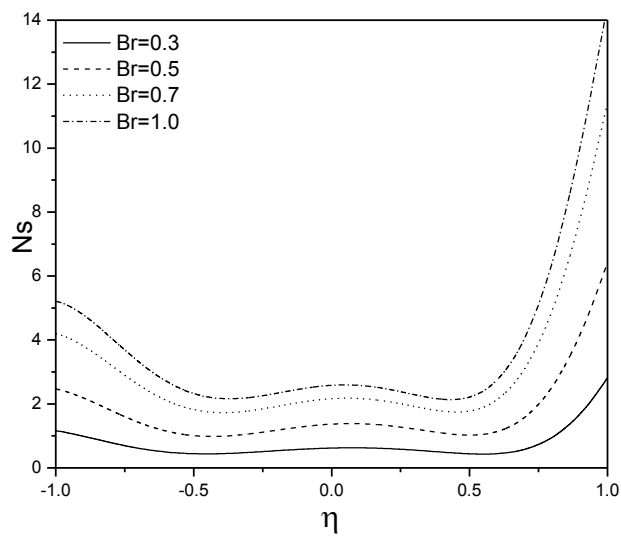


(c) $Ns(\eta)$

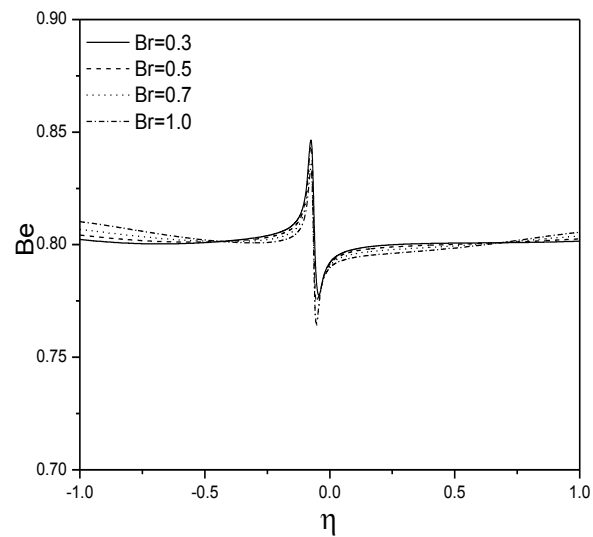


(d) $Be(\eta)$

Figure 6: Effects of magnetic parameter on entropy generation and Bejan number.

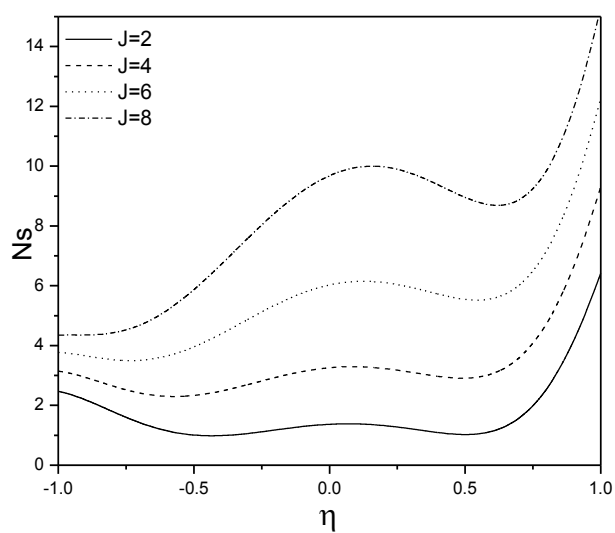


(a) $Ns(\eta)$

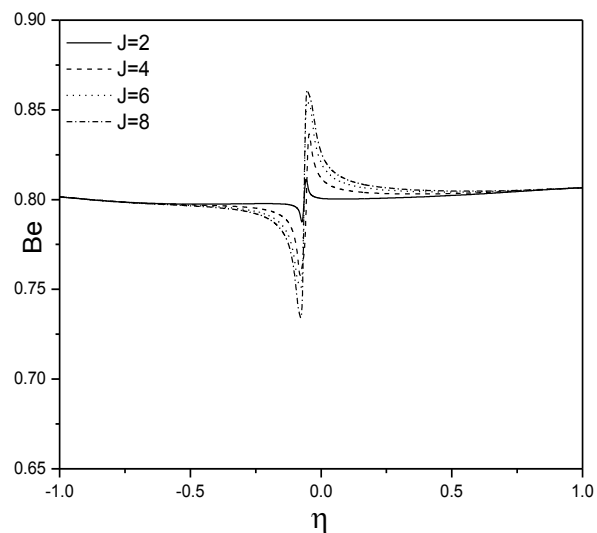


(b) $Be(\eta)$

Figure 7: Effects of Brinkman number on entropy generation and Bejan number



(c) $Ns(\eta)$



(d) $Be(\eta)$

Figure 8: Effects of Joule heating parameter on entropy generation and Bejan number.